



HAL
open science

Charaterization of lipid rafts from *Medicago truncatula* root plasma membranes: a proteomic study reveals the presence of a raft-associated redox system

Benoît Lefebvre, Fabienne Furt, Marie-Andrée Hartmann, Louise V. Michaelson, Jean-Pierre Carde, Françoise Boiron-Sargueil, Michel Rossignol, Johnathan A. Napier, Julie Cullimore, Jean-Jacques Bessoule, et al.

► To cite this version:

Benoît Lefebvre, Fabienne Furt, Marie-Andrée Hartmann, Louise V. Michaelson, Jean-Pierre Carde, et al.. Charaterization of lipid rafts from *Medicago truncatula* root plasma membranes: a proteomic study reveals the presence of a raft-associated redox system. *Plant Physiology*, 2007, 144 (1), pp.402-418. 10.1104/pp.106.094102 . hal-00159551

HAL Id: hal-00159551

<https://hal.science/hal-00159551v1>

Submitted on 29 Dec 2024

HAL is a multi-disciplinary open access archive for the deposit and dissemination of scientific research documents, whether they are published or not. The documents may come from teaching and research institutions in France or abroad, or from public or private research centers.

L'archive ouverte pluridisciplinaire **HAL**, est destinée au dépôt et à la diffusion de documents scientifiques de niveau recherche, publiés ou non, émanant des établissements d'enseignement et de recherche français ou étrangers, des laboratoires publics ou privés.

Characterization of Lipid Rafts from *Medicago truncatula* Root Plasma Membranes: A Proteomic Study Reveals the Presence of a Raft-Associated Redox System^{1[W]}

Benoit Lefebvre, Fabienne Furt, Marie-Andrée Hartmann, Louise V. Michaelson, Jean-Pierre Carde, Françoise Sargueil-Boiron, Michel Rossignol, Johnathan A. Napier, Julie Cullimore, Jean-Jacques Bessoule, and Sébastien Mongrand*

Laboratoire des Interactions Plantes Micro-organismes, Unité Mixte de Recherche, Centre National de la Recherche Scientifique-Institut National de la Recherche Agronomique 2594/441, 31326 Castanet-Tolosan cedex, France (B.L., J.C.); Laboratoire de Biogenèse Membranaire, Unité Mixte de Recherche 5200-Centre National de la Recherche Scientifique-Université Victor Segalen Bordeaux 2, 33076 Bordeaux cedex, France (F.F., F.S.-B., J.-J.B., S.M.); Plate-forme proteomique, IFR40, 31326 Castanet-Tolosan cedex, France (M.R.); Plateau technique Imagerie/Cytologie, Institut National de la Recherche Agronomique, IFR 103, 33883 Villenave d'Ornon cedex, France (J.-P.C.); Institut de Biologie Moléculaire des Plantes, Unité Propre de Recherche-Centre National de la Recherche Scientifique 2357, 67083 Strasbourg cedex, France (M.-A.H.); and Crop Performance and Improvement Division, Rothamsted Research, Harpenden, Hertfordshire AL5 2JQ, United Kingdom (L.V.M., J.A.N.)

Several studies have provided new insights into the role of sphingolipid/sterol-rich domains so-called lipid rafts of the plasma membrane (PM) from mammalian cells, and more recently from leaves, cell cultures, and seedlings of higher plants. Here we show that lipid raft domains, defined as Triton X-100-insoluble membranes, can also be prepared from *Medicago truncatula* root PMs. These domains have been extensively characterized by ultrastructural studies as well as by analysis of their content in lipids and proteins. *M. truncatula* lipid domains are shown to be enriched in sphingolipids and Δ^7 -sterols, with spinasterol as the major compound, but also in steryl glycosides and acyl-steryl glycosides. A large number of proteins (i.e. 270) have been identified. Among them, receptor kinases and proteins related to signaling, cellular trafficking, and cell wall functioning were well represented whereas those involved in transport and metabolism were poorly represented. Evidence is also given for the presence of a complete PM redox system in the lipid rafts.

The plasma membrane (PM) of living cells is known to play a key role in the perception and transduction of signals that regulate the communication of cells with their environment. A model of PM structure has emerged in the past decade from biophysical and biological studies on animal PM in which liquid-ordered domains enriched in cholesterol/sphingolipids coexist with liquid-crystalline domains rich in phospholipids containing unsaturated fatty acids (for review, see Simons and Vaz, 2004). Sterols are thought to

fill the voids between the sphingolipid acyl chains, resulting in an increase of the packing of lipids. Hydrophilic interactions also occur between the hydroxyl groups of the sterols and the sphingolipid acyl chains. Because sphingolipid/cholesterol-rich liposomes were found to be insoluble in mild nonionic detergents such as Triton X-100 (TX100) at 4°C, the analysis of low-density TX100-insoluble membrane fractions were thought to reflect the in vivo composition of lipid microdomains (Brown and Rose, 1992; Schroeder et al., 1994; Simons and Ikonen, 1997; Brown and London, 1998). Consequently, one could assume that the insolubility in cold TX100 and the ability to float on density gradients of a given protein constituted a criterion for its localization or its interaction with these lipid microdomains. These membrane domains were termed lipid rafts by Simons and Ikonen in the late 1990s, a name which rapidly raised their popularity both in mammalian and yeast (*Saccharomyces cerevisiae*) biology (Rajendran and Simons, 2005). Lipid rafts have been proposed to play biological roles in signal transduction (Simons and Toomre, 2000), exocytosis (Salaün et al., 2004), endocytosis (Parton and Richards, 2003), apoptosis (Garcia et al., 2003), and actin cytoskeleton organization (Wickstrom et al., 2003; Falk

¹ This work was supported by Conseil Régional d'Aquitaine, France (to J.-J.B., S.M., F.S.-B., F.F.), and Agence Nationale de la Recherche (to J.C., S.M.). B.L. and F.F. are funded by fellowships from the Ministère délégué à l'Enseignement supérieur et à la Recherche, France.

* Corresponding author; e-mail sebastien.mongrand@biomemb.u-bordeaux2.fr; fax 033-5-56-51-83-61.

The author responsible for distribution of materials integral to the findings presented in this article in accordance with the policy described in the Instructions for Authors (www.plantphysiol.org) is: Sébastien Mongrand (sebastien.mongrand@biomemb.u-bordeaux2.fr).

et al., 2004). In addition, lipid rafts appear to be used for toxin and virus cellular entry (Rosenberger et al., 2000; Lafont et al., 2004) and for viral budding (Brugger et al., 2006). The in vivo occurrence, size, and extent in the PM of lipid rafts are still matters of debate (Munro, 2003). However, intensive work has been performed in some lipid raft proteins such as the T-cell receptor showing that their detergent-insolubility property correlates with functional properties (for review, see He et al., 2005). The emerging use of microscopic analyses to localize proteins in lipid raft and to deduce their lateral mobility should give new insights into in vivo lipid raft protein composition, size, and dynamics (Kenworthy et al., 2004; Douglass and Vale, 2005).

Despite this rising interest, the literature on membrane domains in plant cells is still poorly documented (for review, see Bhat and Panstruga, 2005). To our knowledge, our laboratory was the first to analyze the lipid and the protein content of detergent-insoluble membranes (DIMs) in plants (Mongrand et al., 2004). These DIMs were shown to have certain properties of mammalian and yeast lipid rafts. A protein and lipid characterization was also performed from *Arabidopsis* (*Arabidopsis thaliana*) callus microsomes (Borner et al., 2005). Other studies have identified proteins present in DIMs of *Arabidopsis* leaves and the tobacco (*Nicotiana tabacum*) Bright-Yellow2 (BY2) cell line (Peskan et al., 2000; Shahollari et al., 2004; Morel et al., 2006). The protein composition of the plant DIMs seems to differ from the composition of the PM (Alexandersson et al., 2004; Marmagne et al., 2004), and proteins found suggest roles of these domains in plant defense reactions (Leu-rich repeat receptor-like kinases [LRR-RLKs], remorin, kinases, NADPH oxidase), vectorial water flow (aquaporin), vesicular trafficking (syntaxin, dynamin-like protein), cell growth (proton ATPase), and cytoskeleton organization (actin, tubulin).

This work is devoted to the complete characterization of PM lipid rafts from *Medicago truncatula* roots. Roots are responsible for many important plant functions such as water and nutrient acquisition essential for cellular metabolism and plant growth, adaptation to biotic and abiotic stress such as pathogen attacks, or salt stress. They also form agronomically and environmentally mutualistic interactions with soilborne microorganisms, among which the most widespread are the symbioses with mycorrhizal fungi. The symbiosis with rhizobial bacteria, which is restricted to legumes, is also very important because it leads to atmospheric nitrogen fixation and the growth of these plants without an added nitrogen source. The legume *M. truncatula* has been internationally adopted as a model plant and genomic and EST sequence banks are well developed. The involvement of the root PM in perception, signaling, or exchange with the soil as well as the putative role of lipid rafts as a signaling platform prompted us to characterize lipid rafts from *M. truncatula* root PM. To our knowledge, this study is the first to report the characterization of PM lipid rafts from root tissue.

We isolated a root PM-enriched fraction by phase partition and determined the lipid composition of

DIMs compared with the root PM. Sphingolipids, free sterols, and steryl glycosides (SGs) appeared as the main lipid components of these DIMs. A morphological comparison between PM and DIMs was also carried out, by electronic microscopy, showing the high rigidity of DIMs and their strong ability to undergo self adhesion. A proteomic approach allowed us to identify 270 proteins including numerous proteins that might be involved in cell signaling (RLK, Phospholipase C, remorin, etc) and in an electron transfer system (peroxidase, NADP ubiquinone oxidoreductase, cytochrome b561, L-ascorbate oxidase [AO]).

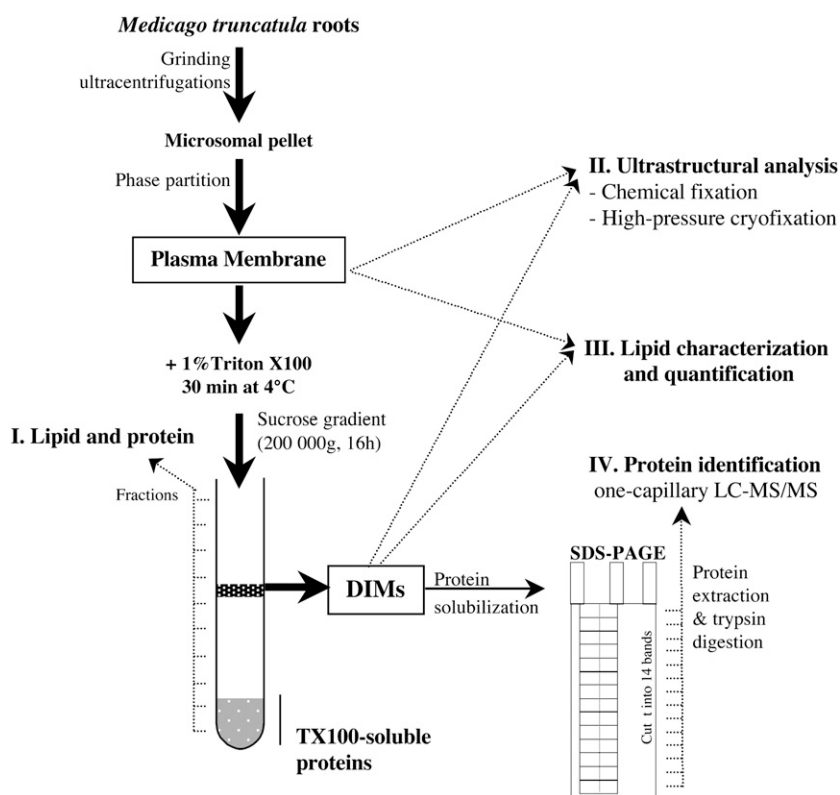
RESULTS

Isolation of PM and DIM from Roots of *M. truncatula*

We used aeroponic cultures of *M. truncatula* plants and the conventional phase-partition procedure to obtain PM-enriched fraction (approximately 500–700 μg protein per 150 g root fresh weight). The purity of the PM fraction was first checked with marker activities to evaluate the contamination by other membranes. Measurement of the vanadate-sensitive ATPase activity showed a 7-fold enrichment in PM proteins after phase partition compared with the starting material consisting of a crude microsomal fraction; a classical ratio for this technique. The mitochondrial marker activity was depleted by a factor of 7.0 between microsomes and PM, and the tonoplast marker by a factor of 5.6 (see Supplemental Table S1). The absence of monogalactosyldiacylglycerol (data not shown) indicated a lack of contamination by plastid envelopes. The purity of the PM fraction was further confirmed by ultrastructural analysis (see below). These results indicate that we could purify a PM-enriched fraction from *Medicago* roots, without significant contaminant by other endomembranes and suitable as starting material for extraction of lipid rafts.

The property of insolubility of particular proteins and lipids in nonionic detergents at low temperature has been commonly used to characterize membrane microdomains called lipid rafts. The *Medicago* root PM fraction was treated for 30 min with 1% cold TX100 with a ratio of detergent-to-protein of 12:1, as previously established (Mongrand et al., 2004). Treated membranes were further submitted to a Suc-discontinuous flotation gradient at 200,000g for 16 h. DIMs were observed as a white and opaque band, below the 30% to 35% Suc interface (Fig. 1). After centrifugation, 10 fractions were collected from the top to the bottom of the gradient (Fig. 2). The protein amount in each fraction was first determined. Fraction numbers 9 to 10 at the bottom of the gradient contained proteins soluble in TX100, which represented up to 88% of the total PM proteins, whereas DIMs represented only 12.0% \pm 2.9% ($n = 3$; Fig. 2). We carried out monodimensional gel electrophoresis to analyze the protein content of the microsomal fraction, PM, and DIMs. We

Figure 1. Strategy used for characterization of *M. truncatula* root PM DIMs.



observed that some proteins were enriched, whereas others were excluded from the DIMs when compared to the PM (data not shown). We examined the distribution of the PM proton pump ATPases (PMAs) found to be associated with other plant DIM fractions (Mongrand et al., 2004; Borner et al., 2005; Morel et al., 2006) and also in *Medicago* DIMs (see Table I). Results presented in Figure 2 show that PMAs are about equally distributed between the DIM fraction and the TX100 soluble fraction. Taking into account the different protein content between the two fractions, this result suggests that PMAs are enriched about 7-fold in *Medicago* root lipid rafts. Lipid analysis of both fractions containing most of the proteins (i.e. fraction nos. 4 and 10) showed that fraction number 4 (DIMs) was enriched in sphingolipids, SGs, and neutral lipids whereas glycerolipids were enriched in fraction number 10 (Fig. 2). We must emphasize that the lipid extraction performed directly on fractions containing a very high amount of Suc (and TX100 in fraction no. 10) do not allow a proper and complete lipid extraction. Therefore, the thin-layer chromatography (TLC) patterns shown in Figure 2 are just an indication of the lipid content of the top and bottom fractions, the extensive lipid analysis of the DIM fraction is shown in Figures 5 to 7.

The DIM fraction was used for further studies and compared to the PM fraction from which it originates (Fig. 1). The study consisted of (1) morphological studies by electron microscopy of isolated fractions after chemical or physical fixation, (2) lipid character-

ization using high performance (HP)-TLC, gas chromatography (GC), and mass spectrometry (MS) analyses, and (3) protein identification by a proteomic-based approach of one-dimensional SDS-PAGE coupled to nano-liquid chromatography (nLC)-electrospray ionization (ESI) analysis.

Ultrastructural Analysis of *Medicago* Root DIMs Compared to PM

Membranes (PM and DIMs) were processed either by chemical fixation or by physical fixation (high-pressure cryofixation followed by freeze substitution). Electron microscopy observations showed that the *Medicago* PM fraction contained mostly membrane vesicles and only a small amount of dense, nonmembranous material. The membrane of vesicles assumed to originate from the PM was thicker (5.5–6 nm) and displayed a heavier electronic contrast. After chemical fixation, the shape and contrast of these vesicles were very variable, some of them appeared to be more or less spherical, whereas others were flattened (Fig. 3, A and C). By contrast, after freeze fixation and substitution most of the vesicles were distinctly ring shaped, with a high electronic contrast, the membrane leaflet being very clearly delineated (Fig. 3, B and D). It has to be noted that no change was observed in regard to apparent membrane thickness when the two methods were compared.

The DIM pellet (Fig. 4) was also processed by chemical fixation or by physical fixation. In both cases, it was

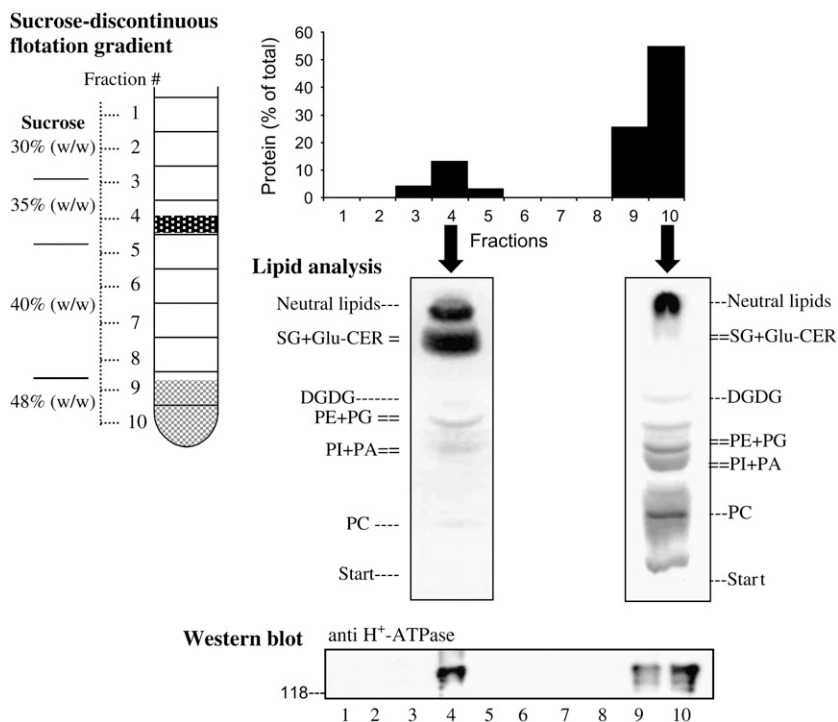


Figure 2. Isolation of DIMs from *Medicago* root PM by discontinuous Suc flotation gradient. PM-enriched fractions (PM) purified from *Medicago* roots were solubilized for 30 min at 4°C with 1% TX100, ratio detergent to proteins of 12:1 (w/w). Treated membranes were submitted to flotation through a Suc density gradient by centrifugation for 16 h at 200,000g. Ten fractions were collected from the top to the bottom. Amounts of proteins were determined by the bicinchoninic acid method. Lipids of fraction numbers 4 (DIMs) and 10 (TX100-soluble fraction) were extracted and analyzed by HP-TLC. Plates were stained with primuline, imaged under UV, and compared to standards. Lipid abbreviations are the following: DGDG, digalactosyldiacylglycerol; PA, phosphatidic acid; PC, phosphatidylcholine; PE, phosphatidylethanolamine; PG, phosphatidylglycerol; PI, phosphatidylinositol; PS, phosphatidyl serine. H⁺-ATPase (PMA) in each fraction was detected by SDS-PAGE and western blotting.

found to contain mostly long membrane fragments, some membrane vesicles, and also aggregates of dense material. After chemical fixation, these components were scattered randomly in the pellet (Fig. 4A). Membrane strips could be seen either as transverse sections or flat views (Fig. 4C), they were not straight edged, but with irregular outlines, 40 to 120 nm wide. The thickness (approximately 6.5 nm) and the electronic contrast of the membranes were constant all along the fragments. After high-pressure fixation, the general organization of the DIM pellet was quite different. The pellet components were not loose but tightly packed and consisted of long, straight membrane fragments, either isolated or densely packed, which appear to stack into onion-like structures (Fig. 4, B and F). This aggregation was probably due to the high pressure during the fixation procedure. Unlike chemically fixed ones, freeze-fixed DIMs appeared to be far less tilted and appeared mostly as cross sections, showing even thickness and contrast and more even width, approximately 50 nm (Fig. 4D). A distinct attention was paid to the dense aggregates, which were clearly seen between membrane fragments. High magnifications showed that they consist of two different elements, namely very small 10 to 15 nm long membrane fragments and discrete clusters of seemingly proteinaceous dense material (Fig. 4E). Taken together our observations showed that DIMs are distinct from the PM vesicles and consist largely of long and narrow, highly rigid, membrane strips. These observations also demonstrated that high-pressure freeze fixation of membrane pellets followed by freeze substitution provides a better definition of membrane shape and contrast compared to chemical fixation.

Polar and Neutral Lipids of *Medicago* PM and DIM Fraction

To investigate the lipid content of PM and DIMs, we first extracted lipids by chloroform:methanol (2:1). The various lipid classes were further separated by HP-TLC with a series of different solvent mixtures. Figure 5A displays HP-TLC plates for the separation of phospholipids (polar lipids 1), SGs (polar lipids 2), and neutral lipids. Acyl-containing lipids of PM and DIM were quantified by densitometric scanning after copper sulfate staining, and by GC analysis after methanolic acid hydrolysis, for sterol-containing lipids. Figure 5B shows that glycerolipids (phospholipids and digalactosyldiacylglycerol) represented up to 50.9% of the total polar lipids in the PM but only 23.8% in DIMs. In contrast, we observed in the DIMs, an enrichment in free sterols (1.7-fold, P value = 0.025), SGs (1.6-fold, P value = 0.001), and acyl-SGs (1.8-fold, P value = 0.019), glucosylceramide being not significantly enriched (1.3-fold, P value = 0.297). Neutral lipid analysis of *Medicago* PM and DIMs showed only two major components, namely free sterols and free fatty acids; sterol esters, triacylglycerol, and monoacylglycerol were not detected (Fig. 5A).

Spinasterol Is the Major Neutral Lipid of *Medicago* Root DIMs

Free phytosterols were 1.7-fold enriched in DIMs compare to PM (Fig. 5B). They were further purified from the plates and analyzed as acetate derivatives by GC. The GC patterns revealed one major component and at least five minor sterols (Fig. 6A). The *Medicago*

Table 1. Signaling proteins

Name and accession number (Acc No.) according to the EST database (Mt...), genomic database (AC...), or to the *Medicago* gene published in NCBI database. When *Medicago* proteins are not annotated, the protein features from the characterized blast entry with the highest score is used. Score, Mascot score ($P < 0.05$ to misidentify an accession when the score is higher than 38 for the EST library, 36 for the genomic library, and 26 for the NCBI database); Pep, number of peptides from the corresponding protein; MW, theoretical M_r in kD; TM, number of transmembrane domains; PTM, posttranslational modifications (myr, myristoylation); SP, signal peptide; Loc, protein localization (according to literature, Psort, or SUBA database), in italics when putative (Cyt, cytoplasm; Nuc, nucleus; ER, endoplasmic reticulum; To, tonoplast; Mit, mitochondria; Pla, plastid; Apo, apoplast; ?, no likely localization). Accessions that share all identified peptides with others containing at least one unique peptide are shown in Supplemental Table S2.

Protein Function (No. of Identified Proteins)	Acc No.	Score	Pep	MW	TM	PTM	SP	Loc
Signaling proteins (43)								
RLKs (31)								
LRR	MtD06341_1	180	4	25.0	1		+	PM
LRR	MtD12384_1	170	5	54.8	1			PM
LRR	AC146586_24.1	107	4	71.5	1			PM
LRR	AC146586_13.1	105	2	55.7	1			PM
LRR	AC137080_18.1	88	3	39.0	2		+	PM
LRR (Arabidopsis), $E = 4e-114$	MtD01112_1	81	2	43.6	1		+	PM
LRR, Cys-containing type	AC133779_2.1	80	2	116.4	1		+	PM
Ser/Thr protein kinase (LRR)	MtC50421_1	70	2	64.6	0			PM
Ser/Thr protein kinase (S-locus)	AC136138_9.1	65	2	38.3	1			PM
LRR (Arabidopsis), $E = 3e-56$	MtD01393_1	64	1	28.3	0		+	PM
LRR	MtD04430_1	64	1	19.3	1		+	PM
Ser/Thr protein kinase (LRR)	AC146586_9.1	63	2	46.4	1			PM
Legume lectin	MtC10055_1	62	1	30.9	1			PM
LRR	MtD01628.1_1	61	1	45.9	1			PM
Disease resistance protein; LRR	AC126790_24.1	58	3	138.0	1			PM
LRR	AC147002_8.1	54	2	105.5	1			PM
LRR	MtD27273_1	50	1	30.4	1			PM
Lectin receptor kinase related	AC148775_5.1	44	1	10.8	0			PM
Ser/Thr protein kinase (LRR)	MtD01246_1	39	2	57.4	1			PM
Ser/Thr protein kinase	MtD05664_1	38	1	47.8	1			PM
DUF26; Ser/Thr protein kinase	AC147431_11.1	37	2	74.9	2		+	PM
Other kinases (4)								
ENOD18 (<i>Vicia faba</i>), $E = 1e-32$	MtD20066_1	133	3	13.8	0			Cyt
EDR1 kinase (Arabidopsis), $E = 2e-174$	AC139526_23.1	58	4	111.7	0			?
Ser/Thr protein kinase	MtD03140_1	41	1	29.0	0			Cyt
Ser/Thr protein kinase	AC151526_16.1	39	3	59.3	0			Cyt
Other signaling proteins (8)								
Cell elongation protein diminuto, fad linked oxidase	MtC20007_1	533	12	65.6	1			PM
Phosphoinositide-specific phospholipase C	AAL17948.1	211	12	67.5	0			PM
Phosphatidylinositol-specific phospholipase C	MtC60898_1	159	4	36.2	0	Myr		PM
Remorin	MtC00278_1	74	2	21.6	0			PM
Remorin, Pro-rich region	MtC60319_1	69	1	23.0	0			PM
Acid phosphatase precursor, metallophosphoesterase	MtC10130_1	87	2	38.2	0			?
LMBR1 integral membrane like (rice), $E = 0.0$	MtC50311_1	74	2	61.4	9			PM
Peptidoglycan-binding LysM	MtC30180_1	35	1	41.5	2	GPI		PM

sterols were quantified by GC and identified by GC-MS (Itoh et al., 1981, 1982) and the structure of the *Medicago* Δ^7 -phytosterols were determined by MS (Fig. 6B). Spinasterol, a Δ^7 -sterol, was by far the major sterol. The other sterols were ergost-7-en- 3β -ol, stigmast-7-en- 3β -ol, and Δ^7 -avenasterol. Δ^5 -Sterols such as stigmasterol, sitosterol, and isofucosterol were also detected. The PM and DIMs were found to contain the same sterols in similar proportions, indicating no selective sorting of the different sterol molecules between the raft and nonraft fractions (Fig. 6C).

Characterization of Polar Lipids from *Medicago* DIMs

Sphingolipids and SGs of PM and DIMs were recovered after mild-alkaline hydrolysis of corresponding

whole lipid extracts. HP-TLC analysis of the alkaline-stable lipids extracted resolved only three bands (Fig. 7A): free fatty acids (resulting from glycerolipid hydrolysis), neutral lipids (i.e. free sterols), and glucosyl ceramide (gluCER) mixed with SG. These two latter lipids were separated from each other by HP-TLC using a solvent mixture able to resolve GluCER and SG molecular species into different groups (Fig. 7B). We used as standards the tobacco leaf PM gluCER, previously characterized by matrix-assisted laser-desorption ionization time of flight (Mongrand et al., 2004). Conventional lipid extraction procedure using chloroform/methanol can underestimate the levels of more complex sphingolipids, e.g. inositolphosphoryl ceramides, glycosyl-inositolphosphoryl ceramides, or glycosyl-inositolphosphoryl ceramide-anchored proteins

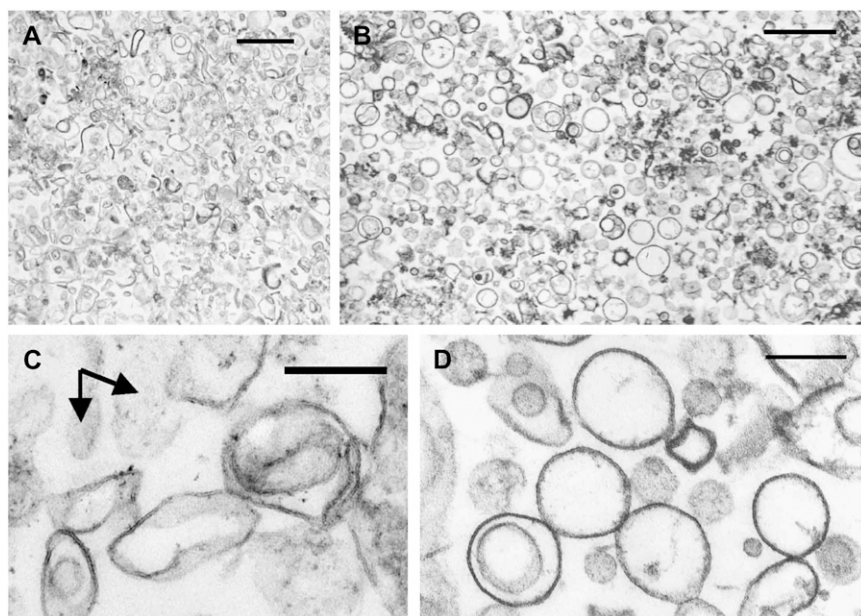


Figure 3. Morphological study of *Medicago* root PM. PM fractions from *Medicago* root was purified as described in experimental procedures. High-speed centrifugation pellets of PM were prepared by chemical fixation (A and C) or high-pressure freeze fixation (B and D) as described in the experimental procedures and observed by transmission electron microscopy. The low abundance of poorly contrasted vesicles (C, arrows) suggests there was no massive contamination of PM by other membrane components. A and B, bar = 1,000 nm; C and D, bar = 200 nm.

because of their very high polarity (Michaelson et al., 2002; Sperling et al., 2005; Markham et al., 2006). In view of these problems, we adopted a direct measurement of total sphingolipids, based on the levels of sphingoid long-chain bases (LCBs) present in either DIM or PM fractions. This approach has previously been successfully used to quantify the levels of sphingolipids in *Arabidopsis* DIM fractions (Borner et al., 2005). Moreover, the ratio of *cis*:*trans* t18:1D8 LCBs has been shown to serve as an estimation of the relative levels of sphingolipids (Sperling et al., 2005). Quantitative measurement of total LCBs in *Medicago* PM and DIMs revealed a 6.7-fold enrichment of sphingolipids in the DIM fraction (Fig. 7C), in excellent agreement with studies on other plant species. Interestingly, although the levels of sphingolipids were increased in the DIM fraction, no significant change in LCB profile was observed. In particular, the *cis*:*trans* ratio of t18:1D8 was unaltered, with the *trans* form being the predominant stereoisomer (>80% of total, see Supplemental Table S4).

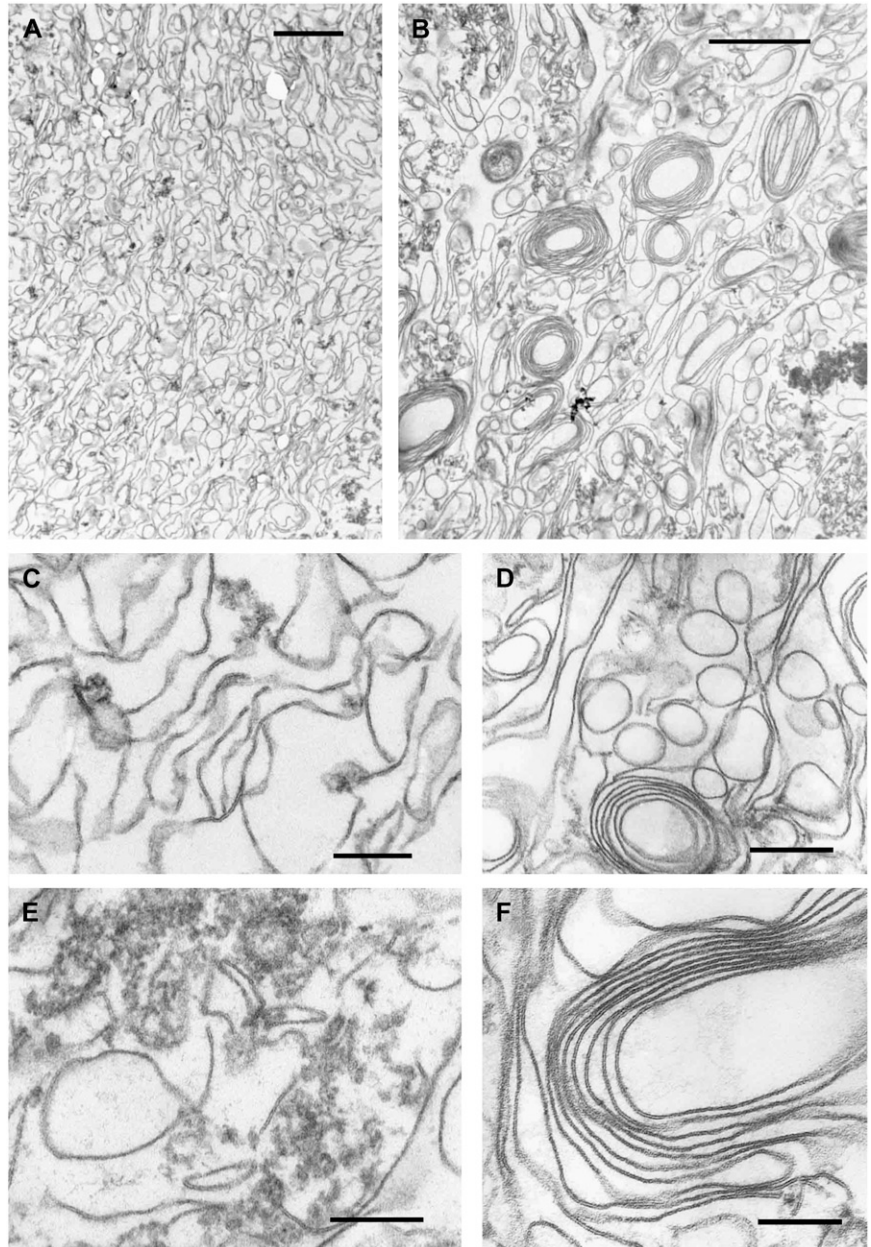
Acylated SGs (ASGs) and SG were 1.6-fold ($P = 0.001$) and 1.8-fold ($P = 0.019$) enriched in DIMs compare to PM. Their position on the HP-TLC plate was determined by comparison with that of commercially available standards. These lipids were also identified due to their pink color after spraying HP-TLC plates with orcinol/sulfuric acid and to their blue color after copper sulfate staining. We further characterized the hydrophobic moieties of SG and ASG (see experimental procedures described in "Materials and Methods"). SG and ASG sterol moieties were quantified by GC. Figure 7D shows that SG and ASG contained the same sterols as the free forms, but in different relative proportions. Thus, the relative amount of Δ^5 -sterols (stigmasterol and sitosterol) in SG and ASG was significantly higher than that in free forms. These results probably indicate

the specificity of steryl-conjugating enzymes to form SG and ASG (Ullmann et al., 1984). Fatty acids present at the 6 position of the monosaccharide of ASG were analyzed and quantified by GC after conversion to the corresponding methyl esters by hot methanolic H_2SO_4 (Fig. 7E). Palmitic acid, C16:0 ($74.2\% \pm 4.6\%$) and stearic acid, C18:0 ($25.2\% \pm 3.6\%$) were found (Fig. 7F).

Proteomic Analysis of DIMs from *Medicago* Root PMs

Proteins copurified with the sphingolipid-sterol-enriched DIM fractions were separated by monodimensional SDS-PAGE. The gel strip was divided into 14 fractions and peptides released by trypsin digestion were analyzed by nLC-ESI using a Q-TRAP mass spectrometer. The peptide sequences deduced from MS were attributed to *M. truncatula* proteins using the MASCOT search engine against either *M. truncatula* EST, genomic, or the National Center for Biotechnology Information (NCBI) databases (see experimental procedures). A total of 270 proteins were identified with this method with a probability of misidentification of <0.05, based on the peptide fragmentation qualities. These 270 proteins were classified as follows: 43 signaling proteins (Table I), 65 transport proteins (Table II), 21 redox proteins (Table III), 30 cytoskeleton, trafficking, and protein-stability factors (Table IV), and 111 miscellaneous proteins including 22 with unknown functions (Table V). For highly related members of multigene families, only the member with the highest mascot score is shown in the tables, with the others being described in Supplemental Table S2. Bioinformatics tools were then used to predict the M_r s, the number of transmembrane domains, the posttranslational addition of a glycosylphosphatidylinositol (GPI) anchor, and the presence of a signal peptide in each of the identified proteins (see experimental procedures),

Figure 4. Morphological study of *Medicago* root DIMs. DIMs from *Medicago* roots were purified as shown in Figure 1. High-speed centrifugation pellets of DIMs were prepared by chemical fixation (A and C) or high-pressure freeze fixation (B and D to F) as described in experimental procedures and observed by transmission electron microscopy. The low power magnification shows the loosened (chemical) versus compact (freeze fixation) organization of the DIMs pellet. A and B, bar = 1,000 nm. C to F, bar = 200 nm.



and results are shown in the different tables. When the subcellular location of a protein was experimentally determined in *Medicago* or other plant species, it is shown in the tables in roman type. If not experimentally determined, the subcellular location of soluble proteins was predicted with Psort and is shown in italics. Predictions of subcellular locations for intrinsic membrane proteins are not reliable and therefore, the putative location of these proteins (shown in italics) is based on suggestions in the literature.

Out of the 43 signaling proteins, 31 of them are RLKs. The proteins have been classified in this family based either on their homology to known RLKs or by the presence of a transmembrane domain linked to either a RLK extracellular or kinase domain. Twenty-one spe-

cific RLK proteins were unambiguously identified through having at least one specific peptide (see Table I). Sixteen RLKs belong to the LRR-RLK families but two representatives of the lectin, one of the *S*-locus, and one of the DUF26 families were also identified. In addition 10 RLK peptides were identified that were common with some of the 21 unambiguously identified RLK proteins but might suggest also the presence of members of the *S*-locus, DUF26, WAK, and LRR families (shown in green in Supplemental Table S2).

Many proteins identified in DIMs are involved in water and nutrient acquisition (Table II). The membrane intrinsic proteins commonly called aquaporins are represented by 17 members (composed of both PIP1 and PIP2 family members). In addition, two phosphate, one

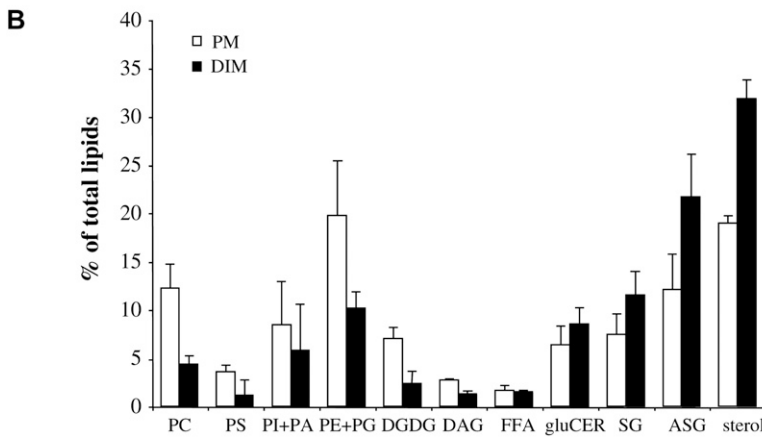
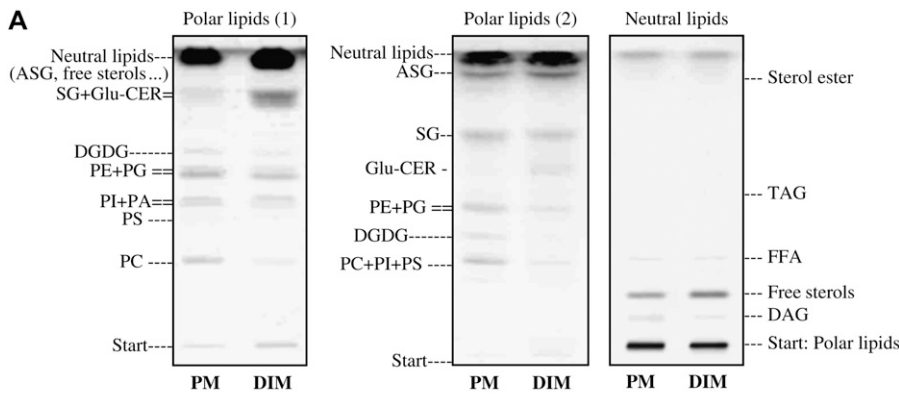


Figure 5. Glycolipid, phospholipid, and neutral lipid analyses of PM and DIMs from *Medicago* roots. DIMs from *Medicago* root PM were purified as shown in Figure 2 (fraction numbers 4 and 5). A, Lipid classes were separated on HP-TLC plates by three different solvent mixtures (see experimental procedures). Plates were stained with primuline and imaged under UV. The identities of lipids were determined by running standards. All free sterols migrated together. B, Lipids of PM and DIM were quantified as described in experimental procedures. The data are expressed as the mean of three independent experiments \pm SD. Lipid abbreviations are the following: DAG, diacylglycerol; DGDG, digalactosyldiacylglycerol; PC, phosphatidylcholine; PE, phosphatidylethanolamine; PG, phosphatidylglycerol; PI, phosphatidylinositol; PS, phosphatidylserine; TAG, triacylglycerol.

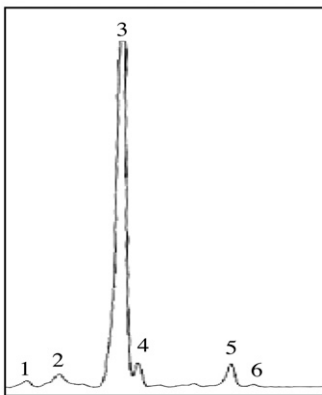
nitrate, and one copper transporter have been identified. Other transport proteins include ion pumps and channels (13 H^+ -ATPases, nine ATP-binding cassette [ABC] transporters, and eight voltage-dependent anion channels).

Several probable integral membrane proteins with a redox activity have been identified (an L-AO, five peroxidases, a cytochrome b561, a germin, and a plastocyanin-like protein). For almost all of them, a signal

peptide has been predicted by the signalP algorithm, suggesting that these proteins follow the secretory pathway and distinguishing them from related mitochondrial or plastidic redox proteins (Table III).

Several isoforms of α and β tubulin (seven proteins), but no other cytoskeleton proteins (i.e. actin) were found in *Medicago* root DIMs. In contrast, a set of trafficking proteins ranging from coat proteins (two clathrins), to

A *Medicago* free sterol GC pattern



B GC/MS characterisation

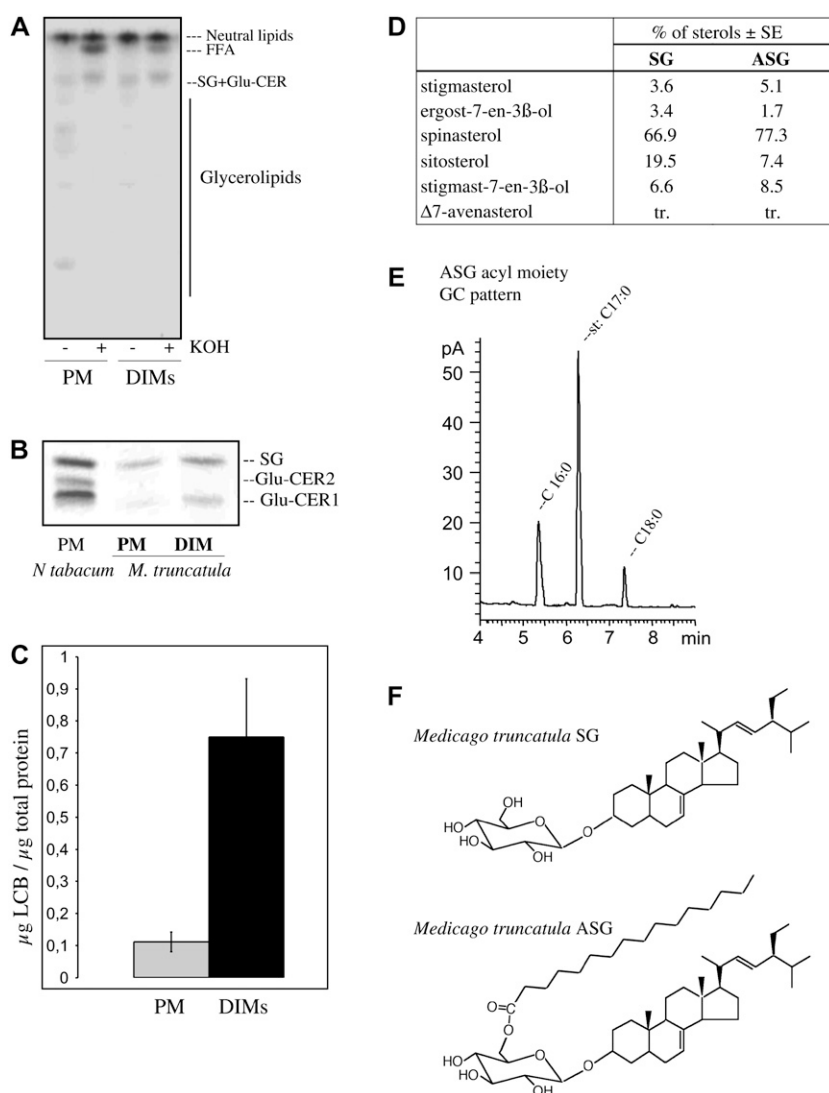
1	Stigmasterol
2	Ergost-7-en-3β-ol m/z 442 (M^+ , 100), 427 (25), 382 (3), 367 (13), 315 (10), 313 (7), 288 (4), 273 (23), 255 (43), 253 (18), 229 (15), 213 (25)
3	Stigmasta-7,22-dien-3β-ol (Spinasterol) m/z 454 (M^+ , 27), 439 (8), 411 (10), 394 (3), 379 (3), 351 (8), 342 (15), 315 (14), 313 (100), 299 (5), 288 (11), 273 (5), 255 (42), 253 (8), 229 (13), 213 (15)
4	Sitosterol
5	Stigmast-7-en-3β-ol m/z 456 (M^+ , 100), 441 (38), 430 (14), 396 (21), 381 (22), 313 (30), 288 (6), 273 (17), 255 (83), 253 (20), 229 (32), 213 (21)
6	Δ^7-avenasterol m/z 454 (M^+), 439 (4), 411 (3), 356 (29), 313 (100), 296 (5), 288 (5), 229 (6), 213 (8), 209 (22)

C

	% of total sterol \pm SE	
	PM	DIM
1 stigmasterol	5.6 \pm 0.6	5.6 \pm 0.3
2 ergost-7-en-3 β -ol	3.1 \pm 0.1	3.1 \pm 0.2
3 stigmasta-7,22-dien-3 β -ol (spinasterol)	84.5 \pm 0.4	84.6 \pm 0.8
4 sitosterol	0.8 \pm 0.1	0.6 \pm 0.1
5 stigmast-7-en-3 β -ol	4.9 \pm 0.3	4.8 \pm 0.1
6 Δ^7 -avenasterol	1.1 \pm 0.4	1.3 \pm 0.3

Figure 6. Sterol composition of DIMs from *Medicago* root PM. DIMs were isolated from *Medicago* root PM and purified as shown in Figure 2. Total lipid extracts were separated on HP-TLC plates and stained with primuline. Free sterols were eluted from the silica gel. They were quantified by GC (A) and identified by GC-MS (B) as acetate derivatives. C, Sterol composition of *Medicago* root PM and DIMs. Cholesterol was used as internal standard. The data are expressed as the mean of three independent experiments \pm SES (SD).

Figure 7. Characterization of lipids from *Medicago* root PM DIMs. A, HP-TLC separation of total lipids from PM and DIMs after mild alkaline hydrolysis. Lipid extracts were solubilized in methanol and treated for 1 h at 80°C in presence or in absence of 2.5 M KOH. B, The mixture SG + GluCER from *Medicago* PMs and DIMs was first purified by HP-TLC (Vitiello and Zanetta, 1978) and further separated each from another by a second HP-TLC according to Hillig et al. (2003). Tobacco GluCER was used as previously characterized standards (Mongrand et al., 2004), mainly composed of glucosylceramide with 4,8-sphingadiene (d18:2^{Δ14,18}) and hydroxypalmitic acid (gluCER1) and of lower amounts of GluCER species with the same backbone but with h18:0, h22:0, and h24:0 fatty acyl chains (gluCER2). C, Sphingolipid LCB content of MP and DIMs expressed as LCB-to-protein ratio (w/w). Results are means ± SES (SD) of three independent MP and DIMs preparations. D, SG and ASG were purified from a *Medicago* PM lipid extract as described above. Corresponding sterol moieties were recovered after acidic hydrolysis and quantified by GC using cholesterol as internal standard (see experimental procedures). The data are expressed as the mean of two independent experiments. E, Fatty acid content of ASG was quantified by GC after conversion to the corresponding methyl esters by methanolic H₂SO₄ at 80°C. The retention times of fatty acid methyl esters were determined by comparison with authentic standards. Fatty acid length and degree of saturation were analyzed qualitatively. A C17 fatty acid was used as internal standard. F, Structures of spinasterol (6'-*O*-palmitoyl)-3β-D-glucopyranoside (SG) and of spinasterol (6'-*O*-palmitoyl)-3β-D-glucopyranoside (ASG), the major sterol conjugates of *Medicago* roots.



coat assembly proteins (four ADP-ribosylation factors), to vesicle fission proteins (a dynamin GTPase effector), to proteins involved in vesicle attachment, to target membranes (a Rab and a prenylated Rab acceptor) were identified. In addition, ubiquitin, linkage of which to PM proteins is known to induce endocytosis and/or proteasome-dependent degradation was found, and classified in Table IV.

Table V regroups all the other identified proteins in the *Medicago* DIMs among which ribosomal proteins represent a large number (50). Among the other proteins identified, six are involved in lipid and six in saccharide (three glycoside hydrolase, an endoglucanase, and two Suc synthases) metabolism (Table V). No function could be attributed to 22 other proteins, because either homologs found with BLASTp have also an unknown function or domain identification by Prodom or Pfam algorithm was unsuccessful. Therefore a putative raft location could give a first indication in search of the functions of these proteins.

Several of the identified proteins belong either to multigenic families (e.g. 17 aquaporins) or to multi-subunit complexes (e.g. tubulin α - and β -chains), thus the 270 proteins represent around 120 functionally distinct proteins or protein complexes. If ribosomal proteins are excluded, half of the identified proteins present in the DIM fraction are predicted to have at least one transmembrane domain or a known β -barrel structure according to TMHMM2 or Pred-TMBB algorithms. Five identified proteins might be attached to the PM by a GPI anchor (Tables I, III, and V), an attachment known to have a high affinity for lipid rafts. Signal peptides have been predicted in 13 proteins that do not seem to be integral membrane proteins, suggesting that they could be extracellular proteins. In the case of proteins identified only in the EST database, sequences are mostly partial, therefore the M_r is usually underestimated and the absence of a signal peptide, GPI anchor, and/or transmembrane domains should be considered with caution.

Table II. *Transport proteins*

For legend see Table I, except that only the isoform or subunit from protein subfamilies or complex subunits with the highest mascot score is shown. For other isoforms or subunits identified, see Supplemental Table S2.

Protein Function (No. of Identified Proteins)	Acc No.	Score	Pep	MW	TM	PTM	SP	Loc
Transport proteins (65)								
Membrane intrinsic proteins (17)								
Aquaporin (PIP1)	AAK66766.1	315	16	30.9	6			PM
P-type H ⁺ -ATPases (8)								
Cation transporting ATPase, E1-E2 type	AC125475_9.1	1,202	32	104.8	9			PM
ABC transporters (9)								
ABC transporter	AC123976_2.1	311	13	167.3	13			To/PM
Transporters (6)								
Phosphate transporter (MTPT1)	AAB81346	228	4	58.8	11			PM
High-affinity nitrate transporter (<i>Arabidopsis</i>), $E = 1e-50$	MtC10028_1	201	4	22.9	1		+	PM
CTR copper transporter	AC137830_15.1	80	2	15.6	3			PM
Monosaccharide/H ⁺ symporter	CAD31121	49	1	55.0	12		+	PM
Mitochondrial substrate carriers (5)								
Mitochondrial substrate carrier	AC149131_13.1	432	9	45.2	3	Myr		Mit
V-type H ⁺ -ATPases (5)								
Vacuolar H ⁺ -ATPase 116 kD subunit (V_0)	MtC40046_1	269	6	92.7	6			To/PM
Voltage-dependent anion channels (8)								
Voltage-dependent anion channel (porin)	AC137994_26.1	368	6	29.6	β -Barrel			Mit/Pla/PM
ATP synthases (3)								
ATP synthase δ -chain (F1)	MtC10318_1	162	3	21.0	0			Mit/PM
Translocon (2)								
Translocon-associated protein, β -subunit precursor	MtC00568_1	66	2	24.8	3		+	ER
Other transport proteins (2)								
Membrane import protein like	AC141922_20.1	59	1	27.8	0			Mit
DUF6; Tpt phosphate/phosphoenolpyruvate translocator	MtD00721_1	67	1	44.5	7			Pla

DISCUSSION

In this study we have used a variety of techniques to characterize the structure, the lipid, and the protein content of lipid rafts from the root PM of the plant model *M. truncatula*. Membrane lipids in plants consist of basically three classes of molecules, namely the diacylglycerol-based lipids, the long-chain-sphingoid-based lipids, and the sterols and their conjugates; these lipids play important roles in determining the physicochemical properties of the biological membranes. Sterols and sphingolipids have been detected as the prominent constituents of lipid rafts from tobacco leaf and BY2 cell PM (Mongrand et al., 2004) and from *Arabidopsis* callus microsomes (Borner et al., 2005). The presence of sterols, glycerolipids, and sphingolipids in root PM (Gronewald et al., 1982) suggest that liquid-ordered (raft) and liquid-crystalline (nonraft) phases could exist in roots. Here we show that DIMs can be isolated from *Medicago* root PM and share some characteristics with the *Arabidopsis* and tobacco lipid rafts. Microscopic examination of purified *Medicago* DIMs show they have a different structure to the PM and consist of long, narrow, and rigid membrane strips, with a lipid bilayer slightly thicker than that of the PM. We must emphasize that the length of isolated DIM strips are too large to reflect the size of membrane domains in vivo, and moreover it has been shown that TX100 treatment triggers aggregation of rafts (Giocondi et al., 2000). Therefore, ultrastructural analysis of iso-

lated DIMs, which reveals a broad size range of membrane strips, are likely to represent a coalescence of smaller raft domains (Shogomori and Brown, 2003).

Free Sterols, Sphingolipids, and SGs Are the Main Lipids of *Medicago* Lipid Rafts

Compared to the PM, *Medicago* root lipid rafts were found to be greatly enriched in sphingolipids, free sterols, and SGs (up to 73.5% of the total raft lipids) and consequently depleted in phospho and glyco glycerolipids (Fig. 5B). Major free sterols of the *Medicago* root PM have been identified as Δ^7 -sterols, with stigmasta-7,22-dien-3 β -ol (spinasterol) as the most represented one (Fig. 6). Δ^5 -Sterols (stigmasterol, sitosterol, and isofucosterol) were also detected. Whereas most higher plants contain Δ^5 -sterols as major sterols, predominance of Δ^7 -sterols appears to be restricted to a few plant families including the Theaceae, Cucurbitaceae, and Sapotaceae (Nes, 1977). The sterol composition of *M. truncatula* roots is similar to that of *Medicago sativa* shoots (Huang and Grunwald, 1988), but differs significantly from that reported for *M. truncatula* cell suspension cultures (Suzuki et al., 2002). As for tobacco or *Arabidopsis* DIMs (Mongrand et al., 2004), *Medicago* root lipid rafts were enriched in free sterols compared to the PM (Fig. 5B). The proportions between the different molecular species were similar to those of the PM, indicating that no selective sorting occurred (Fig. 6C).

Table III. Redox-related proteins

For legend see Table I, except that only the isoform or subunit from protein subfamilies or complex subunits with the highest mascot score is shown. For other isoforms or subunits identified, see Supplemental Table S2.

Protein Function	Acc No.	Score	Pep	MW	TM	PTM	SP	Loc
Redox-related proteins (21)								
NADH-ubiquinone oxidoreductases (4)								
NADH-ubiquinone oxidoreductase (75 kD α -subunit)	MtC00504_1	145	4	80.7	0			Cyt
NADH-ubiquinone oxidoreductase	MtC00519.2_1	130	6	45.1	0		+	?
NADH-ubiquinone oxidoreductase (13 kD α - and β -subunit)	MtC00544_1	83	2	23.8	0			Cyt
NADH-ubiquinone oxidoreductase	MtC20003_1	60	2	26.2	0			Cyt
L-AO (1)								
L-AO	MtC20240_1	161	4	66.3	1	GPI	+	Apo
Peroxidases (5)								
Peroxidase precursor (haem peroxidase)	AC123575_10.1	138	5	36.0	1		+	PM
Dopamine β -monooxygenase domain-containing proteins (2)								
Cytochrome b561, domon domain	AC147406_8.1	244	7	43.5	5			PM
Domon domain	AC126793_22.1	43	2	24.7	2	GPI	+	PM
Other oxidoreductases (9)								
Germin; cupin region	AC149038_25.1	50	1	22.5	0		+	Apo
Plastocyanin like	MtD04199_1	82	2	19.6	2	GPI	+	PM
Ubiquinol-cytochrome c reductase	MtC50199_1	113	3	33.7	0			Mit
Cytochrome bd ubiquinol oxidase (14 kd α -subunit)	MtD22966_1	83	2	14.5	0			Mit
1,4-Benzoquinone reductase	MtC00067_1	266	4	24.0	0			ER/Mit
Cytochrome p450, trans-cinnamate 4-monooxygenase	S36878	109	3	58.1	0			ER
Blue copper-binding protein, plastocyanin like	MtC30578_1	57	1	28.0	0			Pla/PM
Cytochrome c1	AC138464_11.1	63	2	30.9	0		+	?

In *Medicago* root lipid rafts, we have also detected SGs in which the 3 β -hydroxyl group of the sterol is β linked to the 1 position of a monosaccharide, most likely a Glc (data not shown). The presence of an additional fatty acyl chain at the 6 position of the sugar gives rise to ASGs (Fig. 7E). Both types of SGs, which

are common constituents of higher plant membranes (Hartmann and Benveniste, 1987), were found in relative high abundance in *Medicago* root PM, as SG and ASG accounted for about 50% of the total sterols, i.e. as much as the free sterols. The occurrence of SGs have been recently reported in lipid rafts from PM and Golgi

Table IV. Cytoskeleton, trafficking, and protein stability related proteins

For legend see Table I, except that only the isoform or subunit from protein subfamilies or complex subunits with the highest mascot score is shown. For other isoforms or subunits identified, see Supplemental Table S2.

Protein Function (No. of Identified Proteins)	Acc No.	Score	Pep	MW	TM	PTM	SP	Loc
Protein stability (14)								
Ubiquitin (5)								
Ubiquitin domain	CAB96875	79	4	23.6	0			Cyt
Heat shock protein (8)								
Heat shock protein Hsp90	MtD00014_1	97	2	82.7	0			Cyt
Heat shock protein Hsp70	AC140547_7.1	84	3	68.3	0			Cyt
Heat shock protein-related like (rice), $E = 1e-93$	AC148819_7.1	43	3	113.4	0			Cyt
F-box protein (1)								
MtN7 protein	CAA76808	40	1	36.1	0			Cyt
Cytoskeleton (7)								
Tubulins (7)								
Tubulin α -chain	MtC00684_1	62	2	49.8	0			Cyt
Tubulin β -chain	MtC30198_1	126	3	50.0	0			Cyt
Trafficking (9)								
ARF/SAR superfamily (4)								
ADP-ribosylation factor	AAR29293	244	9	20.6	0			Cyt
Clathrin (2)								
Clathrin propeller	AC144729_2.1	199	4	193.2	0			Cyt
Other trafficking proteins (3)								
Phragmoplastin (dynamin GTPase effector)	MtC20035_1	75	2	68.2	0			Cyt
Rab type; ADP-ribosylation factor	MtC60431_1	42	2	29.2	1			?
Prenylated rab acceptor PRA1	MtC10251_1	54	1	23.8	4			?

Table V. Other proteins

For legend see Table I, except that only the isoform or subunit from protein subfamilies or complex subunits with the highest mascot score is shown. For other isoforms or subunits identified, see Supplemental Table S2.

Protein Function (No. of Identified Proteins)	Acc No.	Score	Pep	MW	TM	PTM	SP	Loc
Lipid metabolism (6)								
Glycerophosphoryl diester phosphodiesterase	MtC10375_1	191	4	85.8	1		+	PM
Carnitine	MtC10528_1	143	3	29.3	0			?
Lipoxygenase, LH2 domain	MtD18276_1	69	2	20.0	1		+	?
Lipase/lipoxygenase (<i>M. truncatula</i>), <i>E</i> = 5e-37	MtC50630_1	68	2	21.3	0	GPI	+	PM
C2 domain	MtD13384_1	49	1	21.4	0			?
Patatin	AC125478_14.1	32	1	89.8	0			?
Glycoside hydrolases (3)								
Glycoside hydrolase	AC138016_10.1	217	3	57.7	0			?
Suc synthases (2)								
Suc synthase	CAB40794	139	5	92.3	0			Cyt
Cell wall functioning (2)								
Endo-1,4- β -glucanase	MtC20046_1	208	4	68.9	1			PM
β -lg-H3/fasciclin	MtC93197_1	204	5	28.3	0			PM
Annexin (2)								
Annexin	CAA72183	70	6	37.9	0			?
Elongation factor (3)								
Elongation factor 1a	MtC60291_1	92	3	49.3	0			Cyt
Prohibition (7)								
Band 7 protein	MtD04212_1	493	12	36.1	0			PM
Histone (6)								
Histone H2b	MtC91751_1	117	3	18.0	0			Nuc
Miscellaneous (8)								
β -Hydroxyacyl- <i>acp</i> dehydratase precursor	MtC10913_1	236	4	24.1	0			Pla
Developmentally regulated PM polypeptide	MtC10091_1	199	5	23.8	0			PM
Mitochondrial processing peptidase α -subunit precursor	MtC40075_1	189	4	55.0	0			Mit
Bipartite nuclear localization signal containing protein	MtC30197_1	139	4	45.0	0			Nuc
Insulinase-like peptidase	MtD11663_1	285	6	50.8	0		+	?
Insulinase-like peptidase	MtC60672_1	124	4	42.0	0			?
Calreticulin/calnexin; concanavalin A-like lectin/glucanase	AC139708_17.1	58	2	64.2	2		+	ER
Homocysteine S-methyltransferase	MtD11911_1	52	1	46.0	0			?
Ribosomal proteins (50)								
Ribosomal protein L10e	AC140545_23.1	142	3	25.3	0			Cyt
Proteins of unknown function (22)								

apparatus in leek (*Allium porrum*) and Arabidopsis seedlings (Laloi et al., 2007). In our previous work (Mongrand et al., 2004), we missed these compounds because they migrate at the same place as glucosylceramides. However, we determined that 34% of the so-called gluCER in tobacco leaf lipid rafts readily represent SG (data not shown). In plants, SG participates in the synthesis of cellulose, to produce higher homologs of the cellobioside type with β -1,4-linked glucosyl residues. The resulting disaccharide is split off and used as primer for further elongation to cellulose (Peng et al., 2002). Interestingly, a 1,4- β -glucanase was also found in the *Medicago* DIMs (Table V).

Are SG and ASG Raft Lipids?

Lipid domain-promoting activity of a membrane component is usually considered as its ability to strengthen close packing with saturated lipids (conversely, compounds that impair lipid packing behave as domain-disrupting compounds). Very little attention

has been paid to the effects of SG and ASG on plant membrane properties. One reason is probably the lack of these glycolipids in the PM of mammalian cells. It is expected that SG molecules (Fig. 7F) are oriented in membranes with the sterol moiety embedded in the hydrophobic phase of the bilayer and the sugar in the plane of the polar head groups of the phospholipids. ASGs have probably both the sterol and the fatty acyl chain moieties inside the bilayer and the sugar lying along the hydrophilic surface. In a monolayer system, at a surface pressure of 21 dynes/cm, SG and ASG were found to occupy an area of 38 Å²/mol and 54 Å²/mol, respectively (40 Å²/mol for cholesterol), a result consistent with the hairpin orientation proposed for ASG in the lipid bilayer (Mudd, 1980). Mudd (1980) also showed that both SG and ASG were able to eliminate (ASG) or greatly reduce (SG) the phase transition of dipalmitoyl-phosphatidylcholine liposomes, with the same efficiency as cholesterol or sitosterol. The presence of saturated fatty acyl chains (C16:0 and C18:0) in ASG (Fig. 7E) is consistent with such a hypothesis. The

occurrence of SG and ASG in *Medicago* root lipid rafts raises the question of their physiological roles. Besides the role of SG as a primer for cellulose synthesis (Peng et al., 2002), SG and ASG might modulate the activity of the PM H⁺-ATPase, a protein associated with raft lipids (Mongrand et al., 2004; Bhat and Panstruga, 2005) as they do in the case of the tonoplast H⁺-ATPase (Yamaguchi and Kasamo, 2002). Interestingly, an article has recently reported that SG might act as a mediator in the early stage of stress-responsive signal transduction in human fibroblasts (Kunimoto et al., 2002). It is not unlikely that SG might play a similar role in plant cells.

Proteomic Approach of the Protein Content of *M. truncatula* Root PM Lipid Rafts

Proteins associated with *Medicago* lipid rafts represent about 12% of the total PM protein (Fig. 2), a percentage similar to that observed in tobacco leaves but 2-fold higher than BY2 cells (Morel et al., 2006). By using a combination of peptide extraction and sequencing by MS, we were able to identify 270 proteins in this lipid raft fraction, a much larger number than in most previous studies of plant lipid rafts (Peskan et al., 2000; Mongrand et al., 2004; Shahollari et al., 2004; Borner et al., 2005; Morel et al., 2006). By reference to known proteins and from predictions of the subcellular location of the other proteins it is clear that the lipid raft fraction contains only minor contamination by the ER, the nuclear envelope, and the plastids. Moreover, although several proteins have been identified as mitochondrial or vacuolar, there is evidence that some of these (e.g. ATP synthases [Bae et al., 2004], voltage-dependent anion channels [Bathori et al., 1999], or V-type ATPases [Robinson et al., 1996; Rouquie et al., 1998]) may also have a PM localization. Surprisingly we found a high diversity of ribosomal proteins in the *M. truncatula* DIM fraction (Table V), similar to a previous study on the Arabidopsis PM (Alexandersson et al., 2004). Consistent with a hypothesis from the Arabidopsis work that these proteins may represent ribosomes attached to the cytoskeleton, we also identified α - and β -tubulin in *Medicago* lipid rafts. However, we cannot exclude the possibility that free ribosomes may stick to the raft fractions during extraction (Table IV). It is possible that ribosomes represent the proteinaceous dense material in the *Medicago* DIMs fractions (Fig. 4E).

Our analysis of root lipid rafts identified many proteins that have previously been identified in other lipid rafts (see below). Although our proteome analysis does not establish the enrichment of a protein in the lipid-raft fraction, the identification of these known lipid-raft-associated proteins, coupled with the extensive lipid and structural analyses, suggests that the fraction used for proteomic analysis is highly enriched in lipid rafts. This conclusion is supported by studies on the PM H⁺-ATPases, which was identified in this analysis in addition to previous studies on lipid rafts

of both plants (Mongrand et al., 2004; Borner et al., 2005; Morel et al., 2006) and yeast (Bagnat et al., 2001), and which by western blotting analysis is enriched 7-fold in our root lipid raft fraction in comparison to the PM (Fig. 2). Moreover in this work, often several isoforms of a subfamily or several subunits of a complex were identified, strengthening the functions of these proteins in lipid rafts. Thus the 270 identified proteins represent only 120 functionally distinct proteins or protein complexes and their identity may be used to suggest functions of root lipid rafts.

In Search of Physiological Functions for Lipid Rafts in Root PMs

The major proteins found in *Medicago* root lipid raft are signaling and redox proteins, as well as some subfamilies of pump and channels. In common to other lipid raft studies, we identified aquaporins, ABC transporters, RLKs, remorin, prohibitin, and the PM H⁺-ATPases (Shahollari et al., 2004; Borner et al., 2005; Morel et al., 2006). Moreover, the trafficking proteins clathrin, dynamins, ARE, α - and β -chain of tubulin, RAB, and PRA proteins were identified in the root lipid rafts as previously in their leaf or cell culture counterparts. By contrast with tobacco and Arabidopsis, few soluble protein kinases and G-coupled proteins were detected in *Medicago* lipid rafts. The presence of similar proteins in lipid rafts of different plant tissues and species suggests common function of lipid rafts particularly in signaling, vectorial water uptake, and vesicular trafficking. In addition, this work suggests important roles for lipid rafts that may be specific to roots or that have not previously been identified, as discussed below.

A PM Redox System in *Medicago* Root PM Lipid Rafts

An interesting result of this study is the identification of many proteins belonging to the PM redox system in the *Medicago* root lipid raft (for review, see Vuletic et al., 2005). The NADPH oxidase NtrbohD, previously detected in BY2 lipid rafts (Mongrand et al., 2004) was not found in *Medicago* rafts, but several putative cytosolic NADH-ubiquinone oxidoreductases, a PM integral cytochrome (cyt. b561), and an apoplasm-facing L-AO have all been detected (Table III). These proteins might be involved in electron transfer through the PM and thus in the cytoplasmic and apoplasmic redox balance. In addition, a family of peroxidases with a predicted transmembrane domain and a signal peptide were also detected (Table III). Analysis of the *Medicago* EST database suggests that although present in leaves, most of the ESTs corresponding to these proteins are mainly found in root libraries (<http://medicago.toulouse.inra.fr/Mt/EST/>). In the case of the peroxidases, no EST was found in organs other than roots (see Supplemental Table S3). Production of reactive oxygen species is well known in biotic stress and defense against pathogens. They are also produced as side effects of

abiotic stress such as drought or metal pollution of the soil (for review, see Apel and Hirt, 2004). In particular, apoplastic AO is involved in hormone and pathogen signaling (Pignocchi et al., 2006). In the case of legume-rhizobia interactions, the control of reactive oxygen species production is important during the early steps of symbiosis establishment, both for signaling between the partners and for suppressing plant defense mechanisms (Bueno et al., 2001; Santos et al., 2001; Ramu et al., 2002; Shaw and Long, 2003; Scheidle et al., 2005).

Lipid Rafts, Membrane-Signaling Platform for Root Perception of External Stimuli?

Our data show that many RLKs are present in the root DIM fraction (Table I), strengthening the hypothesis that root lipid rafts, as in animals, are involved in signaling. The RLKs is one of the largest families of plant proteins with about 600 members in Arabidopsis and 1,200 members in rice (*Oryza sativa*; Shiu et al., 2004). The RLKs found in *Medicago* root lipid rafts mainly belong to the LRR subfamily, which is the largest one. Based on their homology to Arabidopsis LRR-RLKs, seven could be classified into subfamily I, four into subfamily VIII, two into subfamily III, and one in each of subfamilies II, X, and XII. Only a few RLKs have been well characterized and none of those that we identified have a known role. The two RLKs from subfamily III, MtD06341 and MtD27273, are the closest homologs of the Arabidopsis At2g26730 and At5g16590 RLKs found previously in Arabidopsis cotyledons lipid rafts (24). Several phosphoinositide-specific phospholipase Cs were found in lipid rafts (Table I); the function of these enzymes in plant signaling has been clearly established, particularly by regulation of Ca²⁺ channels through IP₃ release (Rebecchi and Pentylala, 2000) as well as in the particular case of the signaling during legume-rhizobia interaction (Charron et al., 2004). Finally, ubiquitin and MtN7, proteins involved in targeted-protein degradation, were detected in rafts (Table IV). The cyclin-like F-box protein, MtN7, is likely a component of a ubiquitin-ligase complex involved in signaling via protein degradation and is potentially very interesting, because the gene is up-regulated during establishment of the legume-rhizobia symbiosis (El Yahyaoui et al., 2004).

In conclusion, the work presented here represents a careful and extensive analysis of the structure, lipid, and protein content of lipid rafts from an important plant organ, roots, that had not been characterized previously. The results reveal several novel features of the lipids in these microdomains, and the presence of a redox system, which may be specific to their function in roots. As *M. truncatula* is serving as a model organism for studies on root endosymbioses, these studies will also form a base for future work to examine the role of protein recruitment in plant lipid rafts during symbiotic infection, studies that are complicated by the presence of the two organisms.

MATERIALS AND METHODS

Materials

HP-TLC plates were Silicagel 60 F254 (Merck). Steryl conjugates were purchased from Matreya LLC, other lipid standards and all other reagents were from Sigma.

Plant Material

For each experiment, about 400 plants of *Medicago truncatula* Gaertn 'Jemalong' genotype A17 were grown in an aeroponic chamber for 14 d (22°C; 16 h of light per day) in a nitrogen-rich medium (5 mM NH₄NO₃), then were starved of this nitrogen source for 4 d, as described in Journet et al. (2001). Whole root systems were harvested about 2 cm below the crown.

Preparation and Purity of *M. truncatula* PM

The PM was purified essentially according to Rabotti and Zocchi (1994) and Chiou et al. (2001). All steps were performed at 4°C. Briefly, roots (approximately 150 g) were homogenized in a Waring-blender with 3 volumes of 230 mM sorbitol, 50 mM Tris-HCl pH 7.5, 10 mM KCl, 3 mM EGTA, 20 mM beta-mercaptoethanol, and 1 mM phenylmethylsulfonyl fluoride (PMSF). All buffers were ice cold and the final recovering buffer contained the following protease inhibitors: 0.5 mg/mL leupeptin, 0.7 mg/mL pepstatin, and 0.2 mM PMSF. After filtration, the homogenate was centrifuged for 30 min at 20,000g and the resulting supernatant was centrifuged for 1 h at 100,000g. This microsomal pellet was resuspended in 330 mM sorbitol, 5 mM KCl, 5 mM K₂HPO₄ pH 7.8. PMs were purified twice in an aqueous polymer two-phase system (Larsson et al., 1994) with 21.5 g of phase mixture (6.2% PEG3350 [w/w], 6.2% DextranT-500 [w/w] in 330 mM sorbitol, 5 mM KCl, 5 mM K₂HPO₄ pH 7.8) including 6 g of microsomal fraction. The final upper phase (approximately 500 µg of PM) was diluted with 3 volumes in 4 mL of Tris-buffered saline (TBS) buffer (140 mM NaCl, 3 mM KCl, 25 mM Tris-HCl, pH 7.5) with 1 mM PMSF to remove residual polyethylene glycol-Dextran. After a 35 min centrifugation at 100,000g, the pellet was washed and then resuspended in 0.5 mL of TBS buffer. Protein amount was determined with a Bradford protein assay using bovine serum albumin as standard. PM Vanadate-sensitive ATPase activity was measured in microplates according to Pullman and Penefsky (1976) with 9 mM MgCl₂, 6 mM ATP, 50 mM MES, pH 6.8 0.02% TX100 in each sample for membrane permeabilization. Marker activities used to evaluate the contamination of the PM fraction were: azide-sensitive ATPase activity at pH 9 (for mitochondria) and nitrate-sensitive ATPase activity at pH 8 for (for tonoplasts).

Preparation of DIM

TX100 (10%) was added to a ratio of detergent-to-PM proteins of 10 to 12:1 (in all cases, 1% final concentration), and the membranes were solubilized at 4°C for 30 min, then brought to a final concentration of 52% Suc (w/w), overlaid with successive 3 mL steps of 40%, 35%, and 30% Suc in TBS buffer (w/w), and then centrifuged for 16 h at 200,000g in a TST41 rotor (SORVALL). DIMs could be recovered above the 30% to 35% interface as an opaque band and this fraction was washed in 4 mL of TBS buffer to remove residual Suc. The protein concentration was determined with a bicinchoninic acid protein assay to avoid TX100 interference, using bovine serum albumin as a protein standard.

Electron Microscopy

Purified *Medicago* PM and DIM were pelleted at 100,000g. For chemical fixation, pelleted membranes were sequentially fixed with glutaraldehyde (2.5% in 100 mM phosphate buffer, 2 h at 4°C), osmium tetroxide (1% buffered, 2 h at 4°C), and tannic acid (1% in deionized water, 30 min at 22°C), according to Carde (1987). The pellets were then thoroughly rinsed with water and covered with 2% low melting point agarose, then dehydrated with ethanol and epoxypropane at 22°C and embedded in epon. Other membrane pellets from the same experiment were high-pressure frozen with a Leica EMPACT system. PM and DIM were first layered on a small disc of filter paper inserted in a flat copper carrier, fast frozen, and substituted in acetone containing 1% glutaraldehyde, for 53 h at -90°C. The temperature of the substitution medium was then raised to -60°C (4°C/h over a period of 7 h and 30 min), and maintained at -60°C for 12 h. After rinsing with pure acetone at -60°C (3 times, 10 min), the

substitution medium was replaced by 2% OsO₄ in acetone for 6 h at -60°C, then for 6 h at -30°C (6°C/h over a period of 5 h), raised at 0°C over a period of 6 h (5°C/h), and maintained at 0°C for 4 h. After rinsing in acetone (3 times 10 min), the membrane pellets were treated with 1% tannic acid in acetone, for 1 h at 0°C, then rinsed with acetone (3 times 10 min) and progressively infiltrated with Epon. Sections 50 nm thick were observed with a FEI CM10 electron microscope and digital pictures obtained with a XR60 AMT camera.

Lipid Analysis

Lipids were extracted and purified from the different fractions according to Bligh and Dyer (1959). Phospholipids, glycolipids, and neutral lipids were separated by monodimensional HP-TLC using the solvent systems described by Vitiello and Zanetta (1978), Juguelin et al. (1986), and Yamaguchi and Kasamo (2002), respectively. Lipids were detected by spraying the plates with a solution of 0.1% (w/v) primuline in 80% acetone and imaged under UV light. Lipids of PM and DIM were quantified from HP-TLC plates by densitometric scanning (Macala et al., 1983) from three independent biological samples. Sphingolipids and SGs were recovered by mild alkaline hydrolysis of the total lipid extract for 1 h at 80°C in methanolic 2.5 M KOH. Under these conditions, ASG were converted to SG. SGs and glucosylceramides that comigrated in the Vitiello and Zanetta solvent mixture, were purified from the plates and further separated from each other in chloroform:methanol (85:15 [v/v]) according to Hillig et al. (2003). Glycolipids (SG and ASG) were also purified by silica gel chromatography of a *Medicago* root lipid extract according to Yamaguchi and Kasamo (2002). SGs were separated by HP-TLC using chloroform:methanol: water (85:15:0.5) and identified by their blue color after staining with copper sulfate (Macala et al., 1983). SG and ASG were hydrolyzed by heating in ethanolic 0.8% H₂SO₄ for 4 h. Then sterol moieties of SG and ASG were analyzed as described below. Fatty acids of ASG were determined and quantified by GC after conversion to the corresponding methyl esters by hot methanolic H₂SO₄ according to Browse et al. (1986). The retention times of fatty acid methyl esters were determined by comparison with standards.

Sterols Analysis

Free sterols, SG, and ASG sterol moieties were analyzed by GC as acetate derivatives with a Varian GC model 8300 equipped with a flame ionization detector and a fused capillary column (WCOT 30 m × 0.25 mm i.d.) coated with DB1, with the following program: an initial rise of temperature from 60°C to 220°C at 30°C/min, a rise from 220°C to 280°C at 2°C/min and a plateau at 280°C for 10 min. Cholesterol was used as internal standard. Sterol acetates were identified by GC-MS according to Rahier and Benveniste (1989) and literature data.

LCB Analysis

Total sphingolipid levels were determined by quantitative measurement of sphingolipid LCBs, using methods previously described by Borner et al. (2005). Briefly, total sphingolipids were deacylated by strong alkaline hydrolysis, followed by conversion to dinitrophenol derivatives. Separation, identification, and quantification (via a C20 sphingosine internal standard) were carried out on an Agilent 1100 LC system, with detection of derivatized LCBs by A₃₅₀.

Statistical Analyses

Data are presented in means ± SD from at least three independent experiments from three different biological samples. Comparisons were performed by Student's *t* test and *P* < 0.05 was considered statistically significant.

Protein Separation by SDS-PAGE Electrophoresis

Proteins in the Suc density gradient were precipitated in 10% cold TCA for 30 min at 4°C. After centrifugation the pellet was first washed with 10% TCA in water to remove residual Suc, and finally with cold acetone before being resuspended in Laemli buffer for SDS-PAGE and western-blot analysis.

Western-Blot Analysis

All Antibodies were diluted in TBS-tween supplemented with 1% powdered milk as follows: anti-H⁺-ATPase (Maudoux et al., 2000) 1/20,000; horseradish peroxidase-conjugated secondary antibodies: anti-rabbit (Amer-

sham Pharmacia Biotech) 1/20,000. Detection was performed as described in the ECL western-blotting detection kit (Amersham Pharmacia Biotech).

Proteomic Analysis: In-Gel Protein Digestion

A total of 25 μg of DIMs resuspended in TBS were centrifuged at 100,000g and the pellet was solubilized overnight in 20 μL, 6 M Urea, 2.2 M Thiourea, 5 mM EDTA, 0.1% SDS, 2% *N*-Octyl-Glucoside, 50 mM Tris-HCl pH 8.8. After addition of 13 μL, 4% SDS, 100 mM dithiothreitol, 10% glycerol, 50 mM Tris-HCl pH 8.8, samples were incubated 30 min at room temperature, centrifuged 5 min at 20,000g before protein separation by 1D SDS-PAGE (separating gel: 7.5% acrylamide, stacking gel: 4%). The gel tracks were each cut into 14 slices and the proteins in each slice were digested overnight by 150 ng trypsin as described in Borderies et al. (2003). Peptides were extracted in 40% (v/v) aqueous acetonitrile, 1% (v/v) formic acid, and extracts were reduced to 5 μL by speed-vac evaporation before analysis on the nLC-MS/MS system.

nLC-ESI MS Analysis and Protein Identification

All analysis were performed using a Q-TRAP (LC packings and Applied biosystems/MDS Sciex) nLC-MS/MS system as described in Boudart et al. (2005). Mass data collected during analysis were processed by the Analyst software (Applied Biosystems/MDS Sciex) and the MS/MS lists were used to search the NCBI nonredundant subdatabase "*Medicago truncatula*" and the *M. truncatula* local EST (<http://medicago.toulouse.inra.fr/Mt/EST/>) and genomic databases (<http://www.medicago.org/genome/>) using MASCOT search engine version 2.0. The MASCOT searching parameters were as follows: up to two missed cleavages, 0.5 mass accuracy allowed for parent and the fragment ions, and oxidized Met as variable modification. Probability-based MASCOT scores were used to evaluate protein identifications. Only matches with *P* < 0.05 for random occurrence were considered to be significant. As a general rule, the amount of sequenced peptides per identified protein ranged from one to 16 with an average of three.

In Silico Analysis

Transmembrane domains were predicted by TMHMM2 (<http://www.cbs.dtu.dk/services/TMHMM/>), beta-barrel by Pred-TMBB (<http://biophysic.biol.uoa.gr/PRED-TMBB/>), signal peptide by signalP (<http://www.cbs.dtu.dk/services/SignalP-2.0/>), myristoylation by the MYR Predictor (<http://mendel.imp.ac.at/sat/myristate/SUPLpredictor.htm>), GPI anchor by big-PI Plant Predictor (http://mendel.imp.ac.at/sat/gpi/plant_server.html), subcellular location by Psort (<http://psort.nibb.ac.jp/form.html>) or according to the SUBA database (<http://www.plantenergy.uwa.edu.au/applications/suba>), and protein functional domains by Prodom (<http://prodes.toulouse.inra.fr/prodom/current/html/home.php>).

Supplemental Data

The following materials are available in the online version of this article.

Supplemental Table S1. Specific activities of marker enzymes from various cellular membranes measured in microsomal (μ) or PM fractions from *M. truncatula* roots.

Supplemental Table S2. Accession number: accession number according to the dbEST (Mt...), the International *Medicago* Genome Annotation Group (AC...), or to the NCBI database.

Supplemental Table S3. Percentage (×1,000) of ESTs corresponding to each accession among the total number of ESTs sequenced for cDNA libraries of the indicated organs.

Supplemental Table S4. LCB content of *M. truncatula* root PM and DIM.

ACKNOWLEDGMENTS

MS analysis was performed at the "Plate-forme proteomique, IFR40" with the help of Gisèle Borderies and Carole Pichereaux. Electron microscopic observations were performed at the "Plateau Technique Imagerie/Cytologie, IFR 103," with the skillful collaboration of Martine Peypelut. We are grateful to Jérôme Gouzy and Hélène San Clemente for help with in silico data

analysis and to Alain Puppo for helpful discussion and critical reading of the manuscript. We thank Frederic Domergue for GC analyses and Marc Boutry for anti-H⁺-ATPase antibodies.

Received December 4, 2006; accepted February 20, 2007; published March 2, 2007.

LITERATURE CITED

- Alexandersson E, Saalbach G, Larsson C, Kjellbom P (2004) Arabidopsis plasma membrane proteomics identifies components of transport, signal transduction and membrane trafficking. *Plant Cell Physiol* **45**: 1543–1556
- Apel K, Hirt H (2004) Reactive oxygen species: metabolism, oxidative stress, and signal transduction. *Annu Rev Plant Biol* **55**: 373–399
- Bae TJ, Kim MS, Kim JW, Kim BW, Choo HJ, Lee JW, Kim KB, Lee CS, Kim JH, Chang SY, et al (2004) Lipid raft proteome reveals ATP synthase complex in the cell surface. *Proteomics* **4**: 3536–3548
- Bagnat M, Chang A, Simons K (2001) Plasma membrane proton ATPase Pma1p requires raft association for surface delivery in yeast. *Mol Biol Cell* **12**: 4129–4138
- Bathori G, Parolini I, Tombola F, Szabo I, Messina A, Oliva M, De Pinto V, Lisanti M, Sargiacomo M, Zoratti M (1999) Porin is present in the plasma membrane where it is concentrated in caveolae and caveolae-related domains. *J Biol Chem* **274**: 29607–29612
- Bhat RA, Panstruga R (2005) Lipid rafts in plants. *Planta* **223**: 1–15
- Bligh EG, Dyer WJ (1959) A rapid method of total lipid extraction and purification. *Can J Biochem Physiol* **37**: 911–917
- Borderies G, Jamet E, Lafitte C, Rossignol M, Jauneau A, Boudart G, Monsarrat B, Esquerre-Tugaye MT, Boudet A, Pont-Lezica R (2003) Proteomics of loosely bound cell wall proteins of *Arabidopsis thaliana* cell suspension cultures: a critical analysis. *Electrophoresis* **24**: 3421–3432
- Borner GH, Sherrier DJ, Weimar T, Michaelson LV, Hawkins ND, Macaskill A, Napier JA, Beale MH, Lilley KS, Dupree P (2005) Analysis of detergent-resistant membranes in Arabidopsis: evidence for plasma membrane lipid rafts. *Plant Physiol* **137**: 104–116
- Boudart G, Jamet E, Rossignol M, Lafitte C, Borderies G, Jauneau A, Esquerre-Tugaye MT, Pont-Lezica R (2005) Cell wall proteins in apoplastic fluids of *Arabidopsis thaliana* rosettes: identification by mass spectrometry and bioinformatics. *Proteomics* **5**: 212–221
- Brown DA, London E (1998) Structure and origin of ordered lipid domains in biological membranes. *J Membr Biol* **164**: 103–114
- Brown DA, Rose JK (1992) Sorting of GPI-anchored proteins to glycolipid-enriched membrane subdomains during transport to the apical cell surface. *Cell* **68**: 533–544
- Browse J, McCourt PJ, Somerville CR (1986) Fatty acid composition of leaf lipids determined after combined digestion and fatty acid methyl ester formation from fresh tissue. *Anal Biochem* **152**: 141–145
- Brugger B, Glass B, Haberkant P, Leibrecht I, Wieland FT, Krausslich HG (2006) The HIV lipidome: a raft with an unusual composition. *Proc Natl Acad Sci USA* **103**: 2641–2646
- Bueno P, Soto MJ, Rodriguez-Rosales MP, Sanjuan J, Olivares J, Donaire JP (2001) Time-course of lipoxygenase, antioxidant enzyme activities and H₂O₂ accumulation during the early stages of Rhizobium-legume symbiosis. *New Phytol* **152**: 91–96
- Carde JP (1987) Electron microscopy of plant cell membranes. *In* L Packer, R Douce, eds, *Plant Cell Membranes a Vol. of Methods in Enzymology*, Vol 148. Academic Press, San Diego, pp 599–622
- Charron D, Pingret JL, Chabaud M, Journet EP, Barker DG (2004) Pharmacological evidence that multiple phospholipid signaling pathways link Rhizobium nodulation factor perception in *Medicago truncatula* root hairs to intracellular responses, including Ca²⁺ spiking and specific ENOD gene expression. *Plant Physiol* **136**: 3582–3593
- Chiou TJ, Liu H, Harrison MJ (2001) The spatial expression patterns of a phosphate transporter (MtPT1) from *Medicago truncatula* indicate a role in phosphate transport at the root/soil interface. *Plant J* **25**: 281–293
- Douglass AD, Vale RD (2005) Single-molecule microscopy reveals plasma membrane microdomains created by protein-protein networks that exclude or trap signaling molecules in T cells. *Cell* **121**: 937–950
- El Yahyaoui F, Kuster H, Ben Amor B, Hohnjec N, Puhler A, Becker A, Gouzy J, Vernie T, Gough C, Niebel A, et al (2004) Expression profiling in *Medicago truncatula* identifies more than 750 genes differentially expressed during nodulation, including many potential regulators of the symbiotic program. *Plant Physiol* **136**: 3159–3176
- Falk J, Thoumine O, Dequidt C, Choquet D, Faivre-Sarrailh C (2004) NrCAM coupling to the cytoskeleton depends on multiple protein domains and partitioning into lipid rafts. *Mol Biol Cell* **15**: 4695–4709
- Garcia A, Cayla X, Fleischer A, Guernon J, Alvarez-Franco Canas F, Rebollo MP, Roncal F, Rebollo A (2003) Rafts: a simple way to control apoptosis by subcellular redistribution. *Biochimie* **85**: 727–731
- Giocondi MC, Vie V, Lesniewska E, Goudonnet JP, Le Grimellec C (2000) *In situ* imaging of detergent-resistant membranes by atomic force microscopy. *J Struct Biol* **131**: 38–43
- Gronewald JW, Aboukhalil W, Weber EJ, Hanson JB (1982) Lipid composition of a plasma-membrane enriched fraction of maize roots. *Phytochemistry* **21**: 859–862
- Hartmann M-A, Benveniste P (1987) Plant membrane sterols: isolation, identification and biosynthesis. *Methods Enzymol* **148**: 632–650
- He HT, Lellouch A, Marguet D (2005) Lipid rafts and the initiation of T cell receptor signaling. *Semin Immunol* **17**: 23–33
- Hillig I, Leipelt M, Ott C, Zahringer U, Warnecke D, Heinz E (2003) Formation of glucosylceramide and sterol glucoside by a UDP-glucose-dependent glucosylceramide synthase from cotton expressed in *Pichia pastoris*. *FEBS Lett* **553**: 365–369
- Huang L, Grunwald C (1988) Effect of light on sterol changes in *Medicago sativa*. *Plant Physiol* **88**: 1403–1406
- Itoh T, Kikuchi Y, Tamura T, Matsumoto T (1981) Co-occurrence of chondrillasterol and spinasterol in two cucurbitaceae seeds as shown by ¹³C NMR. *Phytochemistry* **20**: 761–764
- Itoh T, Yoshida K, Tamura T, Matsumoto T (1982) Co-occurrence of C-24 epimeric 24-ethyl- Δ^7 -sterols in the roots of *Trichosanthes japonica*. *Phytochemistry* **21**: 727–730
- Journet EP, El-Gachtouli N, Vernoud V, de Billy F, Pichon M, Dedieu A, Arnould C, Morandi D, Barker DG, Gianinazzi-Pearson V (2001) *Medicago truncatula* ENOD11: a novel RPRP-encoding early nodulin gene expressed during mycorrhization in arbuscule-containing cells. *Mol Plant Microbe Interact* **14**: 737–748
- Juguelin H, Heape A, Boiron F, Cassagne C (1986) A quantitative developmental study of neutral lipids during myelinogenesis in the peripheral nervous system of normal and trembler mice. *Brain Res* **390**: 249–252
- Kenworthy AK, Nichols BJ, Rimmert CL, Hendrix GM, Kumar M, Zimmerberg J, Lippincott-Schwartz J (2004) Dynamics of putative raft-associated proteins at the cell surface. *J Cell Biol* **165**: 735–746
- Kunimoto S, Murofushi W, Kai H, Ishida Y, Uchiyama A, Kobayashi S, Murofushi H, Murakami-Murofushi K (2002) Steryl glucoside is a lipid mediator in stress-responsive signal transduction. *Cell Struct Funct* **27**: 157–162
- Lafont F, Abrami L, van der Goot FG (2004) Bacterial subversion of lipid rafts. *Curr Opin Microbiol* **7**: 4–10
- Laloi M, Perret AM, Chatre L, Melsner S, Cantrel C, Vaultier MN, Zachowski A, Bathany K, Schmitter JM, Vallet M, et al (2007) Insights into the role of specific lipids in the formation and delivery of lipid microdomains to the plasma membrane of plant cells. *Plant Physiol* **143**: 461–472
- Larsson C, Sommarin M, Widell S (1994) Isolation of highly purified plant plasma membranes and separation of inside-out and right-side-out vesicles. *In* H Walter, G Johansson, eds, *Aqueous Two-Phase Systems*, Vol 228. Academic Press, San Diego, pp 451–459
- Macala LJ, Yu RK, Ando S (1983) Analysis of brain lipids by high performance thin-layer chromatography and densitometry. *J Lipid Res* **24**: 1243–1250
- Markham JE, Li J, Cahoon EB, Jaworski JG (2006) Separation and identification of major plant sphingolipid classes from leaves. *J Biol Chem* **281**: 22684–22694
- Marmagne A, Rouet MA, Ferro M, Rolland N, Alcon C, Joyard J, Garin J, Barbier-Brygoo H, Ephritikhine G (2004) Identification of new intrinsic proteins in Arabidopsis plasma membrane proteome. *Mol Cell Proteomics* **3**: 675–691
- Maudoux O, Batoko H, Oecking C, Gevaert K, Vandekerckhove J, Boutry M, Morsomme P (2000) A plant plasma membrane H⁺-ATPase expressed in yeast is activated by phosphorylation at its penultimate residue and binding of 14-3-3 regulatory proteins in the absence of fusicoccin. *J Biol Chem* **275**: 17762–17770
- Michaelson LV, Longman AJ, Sayanova O, Stobart AK, Napier JA (2002) Isolation and characterization of a cDNA encoding a Delta8 sphingo-

- lipid desaturase from *Aquilegia vulgaris*. *Biochem Soc Trans* **30**: 1073–1075
- Mongrand S, Morel J, Laroche J, Claverol S, Carde JP, Hartmann MA, Bonneau M, Simon-Plas F, Lessire R, Bessoule JJ** (2004) Lipid rafts in higher plant cells: purification and characterization of Triton X-100-insoluble microdomains from tobacco plasma membrane. *J Biol Chem* **279**: 36277–36286
- Morel J, Claverol S, Mongrand S, Furt F, Fromentin J, Bessoule JJ, Blein JP, Simon-Plas F** (2006) Proteomics of plant detergent resistant membranes. *Mol Cell Proteomics* **5**: 1396–1411
- Mudd JB** (1980) The biochemistry of plants, a comprehensive treatise. In PK Stumph, EE Conn, eds, *Lipids: Structure and Function*, Vol 4. Sterol Interconversion. Academic Press, New York, pp 509–532
- Munro S** (2003) Lipid rafts: elusive or illusive? *Cell* **115**: 377–388
- Nes W** (1977) The biochemistry of plant sterols. *Adv Lipid Res* **15**: 233–324
- Parton RG, Richards AA** (2003) Lipid rafts and caveolae as portals for endocytosis: new insights and common mechanisms. *Traffic* **4**: 724–738
- Peng L, Kawagoe Y, Hogan P, Delmer D** (2002) Sitosterol-beta-glucoside as primer for cellulose synthesis in plants. *Science* **295**: 147–150
- Peskan T, Westermann M, Oelmüller R** (2000) Identification of low-density Triton X-100-insoluble plasma membrane microdomains in higher plants. *Eur J Biochem* **267**: 6989–6995
- Pignocchi C, Kiddle G, Hernandez I, Foster SJ, Asensi A, Taybi T, Barnes J, Foyer CH** (2006) Ascorbate-oxidase-dependent changes in the redox state of the apoplast modulate gene transcript accumulation leading to modified hormone signaling and orchestration of defense processes in tobacco. *Plant Physiol* **141**: 423–435
- Pullman ME, Penefsky HS** (1963) Preparation and assay of phosphorylating submitochondrial systems: mechanically ruptured mitochondria. *Methods Enzymol* **6**: 277–284
- Rabotti G, Zocchi G** (1994) Plasma membrane-bound H⁺-ATPase and reductase activities in Fe-deficient cucumber roots. *Physiol Plant* **90**: 779–785
- Rahier A, Benveniste P** (1989) Mass spectral identification of phytosterols. In WD Nes, E Parish, eds, *Analysis of Sterols and Other Significant Steroids*. Academic Press, New York, pp 223–250
- Rajendran L, Simons K** (2005) Lipid rafts and membrane dynamics. *J Cell Sci* **118**: 1099–1102
- Ramu SK, Peng HM, Cook DR** (2002) Nod factor induction of reactive oxygen species production is correlated with expression of the early nodulin gene rip1 in *Medicago truncatula*. *Mol Plant Microbe Interact* **15**: 522–528
- Rebecchi MJ, Pentyala SN** (2000) Structure, function, and control of phosphoinositide-specific phospholipase C. *Physiol Rev* **80**: 1291–1335
- Robinson DG, Haschke HP, Hinz G, Hoh B, Maeshima M, Marty F** (1996) Immunological detection of tonoplast polypeptides in the plasma membrane of pea cotyledons. *Planta* **198**: 95–103
- Rosenberger CM, Brumell JH, Finlay BB** (2000) Microbial pathogenesis: lipid rafts as pathogen portals. *Curr Biol* **10**: 823–825
- Rouquie D, Tournaire-Roux C, Szponarski W, Rossignol M, Dumas P** (1998) Cloning of the V-ATPase subunit G in plant: functional expression and sub-cellular localization. *FEBS Lett* **437**: 287–292
- Salaün C, James DJ, Chamberlain LH** (2004) Lipid rafts and the regulation of exocytosis. *Traffic* **5**: 255–264
- Santos R, Herouart D, Sigaud S, Touati D, Puppo A** (2001) Oxidative burst in alfalfa-*Sinorhizobium meliloti* symbiotic interaction. *Mol Plant Microbe Interact* **14**: 86–89
- Scheidle H, Gross A, Niehaus K** (2005) The lipid A substructure of the *Sinorhizobium meliloti* lipopolysaccharides is sufficient to suppress the oxidative burst in host plants. *New Phytol* **165**: 559–565
- Schroeder R, London E, Brown DA** (1994) Interactions between saturated acyl chains confer detergent resistance on lipids and glycosylphosphatidylinositol (GPI)-anchored proteins: GPI-anchored proteins in liposomes and cells show similar behavior. *Proc Natl Acad Sci USA* **91**: 12130–12134
- Shahollari B, Peskan-Berghöfer T, Oelmüller R** (2004) Receptor kinases with leucine-rich repeats are enriched in Triton X-100 insoluble plasma membrane microdomains from plants. *Physiol Plant* **122**: 397–403
- Shaw SL, Long SR** (2003) Nod factor inhibition of reactive oxygen efflux in a host legume. *Plant Physiol* **132**: 2196–2204
- Shiu SH, Karlowski WM, Pan RS, Tzeng YH, Mayer KFX, Li WH** (2004) Comparative analysis of the receptor-like kinase family in Arabidopsis and rice. *Plant Cell* **16**: 1220–1234
- Shogomori H, Brown DA** (2003) Use of detergents to study membrane rafts: the good, the bad, and the ugly. *Biol Chem* **384**: 1259–1263
- Simons K, Ikonen E** (1997) Functional rafts in cell membranes. *Nature* **387**: 569–572
- Simons K, Toomre D** (2000) Lipid rafts and signal transduction. *Nat Rev Mol Cell Biol* **1**: 31–39
- Simons K, Vaz WL** (2004) Model systems, lipid rafts, and cell membranes. *Annu Rev Biophys Biomol Struct* **33**: 269–295
- Sperling P, Franke S, Luthje S, Heinz E** (2005) Are glucocerebrosides the predominant sphingolipids in plant plasma membranes. *Plant Physiol Biochem* **43**: 1031–1038
- Suzuki H, Achnine L, Xu R, Matsuda SP, Dixon RA** (2002) A genomics approach to the early stages of triterpene saponin biosynthesis in *Medicago truncatula*. *Plant J* **32**: 1033–1048
- Ullmann P, Rimmel D, Benveniste P, Bouvier-Navé P** (1984) Phospholipid-dependence of plant UDP-Glucose-beta-D-glucosyltransferase. II. Acetone-mediated delipidation and kinetic studies. *Plant Sci Lett* **36**: 29–36
- Vitiello F, Zanetta JP** (1978) Thin-layer chromatography of phospholipids. *J Chromatogr* **166**: 637–640
- Vuletic M, Sukalovic VH, Vucinic Z** (2005) The coexistence of the oxidative and reductive systems in roots: the role of plasma membranes. *Ann N Y Acad Sci* **1048**: 244–258
- Wickstrom SA, Alitalo K, Keski-Oja J** (2003) Endostatin associates with lipid rafts and induces reorganization of the actin cytoskeleton via down-regulation of RhoA activity. *J Biol Chem* **278**: 37895–37901
- Yamaguchi M, Kasamo K** (2002) Modulation of proton pumping across proteoliposome membranes reconstituted with tonoplast H⁺-ATPase from cultured rice (*Oryza sativa* L. var. Boro) cells by acyl steryl glucoside and steryl glucoside. *Plant Cell Physiol* **43**: 816–822